

BEM3D: a free adaptive fast multipole boundary element library

M. J. Carley

February 3, 2022

Abstract

The design, implementation and analysis of a free library for boundary element calculations is presented. The library is free in the sense of the GNU General Public Licence and is intended to allow users to solve a wide range of problems using the boundary element method. The library incorporates a fast multipole method which is tailored to boundary elements of order higher than zero, taking account of the finite extent of the elements in the generation of the domain tree. The method is tested on a sphere and on a cube, to test its ability to handle sharp edges, and is found to be accurate, efficient and convergent.

1 INTRODUCTION

The boundary element method has become accepted as a standard computational technique for many problems and, when combined with a fast multipole method, it has proven capable of solving very large problems, primarily in scattering calculations for acoustic and electromagnetic applications. This paper describes BEM3D, a free library released under the GNU General Public Licence, for the solution of general problems using the boundary element method, incorporating a fast multipole method which is tailored to boundary element problems using higher-order elements.

Free software has become an important part of the resources available to those working in scientific and computational fields over the last few years. Standard codes and libraries for many of the operations routinely carried out in computation are now freely available and, because their source code is openly published, they can be modified and improved by experts in the field. Because codes are distributed as libraries for a specific purpose, it is possible to select modules which can be combined

in codes for particular applications. This avoids the problem of reinventing the wheel, speeding code development and improving reliability.

The library described in this paper makes use of a number of existing free libraries [1–3] for computational applications, as well as a standard library of portability and utility functions. The existing software is extended by adding functions for the handling of boundary elements, for fast multipole calculations and some support for parallel systems. The intention is that other users will be able to make use of BEM3D to solve their own problems by adding a Green’s function for the partial differential equation in question. This paper describes the design choices which have been made in BEM3D and the implementation of certain features including a novel adaptive fast multipole method for boundary elements.

2 BASIC CODE STRUCTURE

The boundary element library, BEM3D, has been written with a number of goals in mind. The first of these is generality: users should be able to solve different physical problems and implement different solution techniques and elements as required. The second is that existing wheels should be used rather than being reinvented: the codes use other, high-quality, free libraries for various aspects of the work. These are the GNU Triangulated Surface library (GTS) for geometry handling [1], the GNU Scientific Library [2], LAPACK [3] in the iterative solver and the GLIB library for portability functions and special data structures, such as the tree used in the fast multipole method. The GMSH suite of meshing and visualization tools [4] is used to generate geometries and examine results. Using existing free software improves code reliability and gives users an automatic upgrade as these codes are improved.

The library and its programs have been written in C, partly because C is nearly universally supported across the range of computing platforms, partly because the other libraries used have C interfaces, and also because C allows the use of programming techniques which make extension and customization easier, for example, through the use of loadable modules, an approach which is supported by the GLIB library. The resulting code has been written as a number of separate libraries to facilitate code re-use and to encourage generality in the coding.

2.1 Problem definition

For computational purposes, the partial differential equation for a problem is defined by its Green’s function. Boundary integral equations have been applied in many areas of engineering and science and here we concentrate on the Laplace and Helmholtz

potential problems which have applications in fluid dynamics [5] and in acoustic scattering [6, 7]. The form of the integral equation is identical in each case, with only the Green's function being different. For an unbounded domain containing surface(s) S with outward pointing normal \mathbf{n} , the potential ϕ is given by:

$$C(\mathbf{x})\phi(\mathbf{x}) = \int_S G \frac{\partial \phi}{\partial n_1} - \phi \frac{\partial G}{\partial n_1} dS, \quad G = \frac{1}{4\pi R} \quad (1a)$$

$$C(\mathbf{x})\phi(\mathbf{x}) = \int_S G \frac{\partial \phi}{\partial n_1} - \phi \frac{\partial G}{\partial n_1} dS, \quad G = \frac{e^{jkR}}{4\pi R}, \quad (1b)$$

where $k = \omega/c$ is the wavenumber of the Helmholtz problem, $R = |\mathbf{x} - \mathbf{x}_1|$ and subscript 1 denotes variables of integration. The constant C depends on the field point position \mathbf{x} :

$$C(\mathbf{x}) = \begin{cases} 0 & \mathbf{x} \text{ inside } S; \\ 1 & \mathbf{x} \text{ outside } S; \\ 1 + \int_S \frac{\partial G_0}{\partial n_1} dS & \mathbf{x} \text{ on } S \end{cases} \quad (2)$$

with $G_0 = 1/4\pi R$. When \mathbf{x} is on S with the boundary condition $\chi = \partial\phi/\partial n$ prescribed, Equation 1 is a boundary integral equation for ϕ and can be solved using the boundary element method.

The geometry S is discretized into a number of elements with given nodes \mathbf{x}_i , $i = 1, \dots, N$ and interpolation (shape) functions L_i . This yields the system of equations:

$$\sum_{j=1}^N A_{ij}\phi_j = \sum_{j=1}^N B_{ij}\chi_j, \quad (3)$$

with

$$\begin{aligned} A_{ij} &= C_{ij} + \sum_m \int L_j \frac{\partial G}{\partial n_1} dS_m, \\ C_{ij} &= \begin{cases} 1 + \int \partial G_0 / \partial n_1 dS, & i = j \\ 0, & i \neq j, \end{cases} \\ B_{ij} &= \sum_m \int L_j G dS_m, \end{aligned}$$

where the summation over m is taken on elements which contain collocation point j , the shape function L_j is the shape function on element m corresponding to point

j and S_m is the surface of element m . Conceptually, the boundary element method consists of discretizing the surface, assembling the matrices A and B , and solving the system of Equation 3. In practice, as we shall see below, this is not necessarily a feasible approach for large problems, but it is the default method and one which can be used as a baseline for assessing other techniques.

In BEM3D, the integrations in assembling the matrices are performed using quadrature rules for singular integrands [8], Hayami’s transformation for near-singular integrals [9] and the symmetric rules of Wandzura and Xiao [10]. The system is solved using a library, SISL, based on LAPACK [3], which implements the ‘templates’ of Barrett et. al [11]. The solver library allows for parallel solution of problems using the MPI standard and also has a matrix-free option for use with fast-multipole methods, as described below, §3.

2.2 Element types

Within the code of BEM3D, elements are represented as a collection of triangles, based on the underlying GTS triangle data type. This raises the question of how to link computational information to geometric while retaining the freedom to introduce new element types. Previous work using GTS surfaces [12–14] introduced a new data type for the vertices which allowed them to have an integer index which could be used in assembling the system matrices. This is not a satisfactory solution, however, when more general elements are to be implemented. The first reason is that only linear triangular elements based on the underlying triangles can be used; the second is that there is no good way to introduce discontinuities at sharp edges, an essential part of representing general geometries.

The solution which has been adopted is shown in Figure 1. Within the library, an element is composed of a list of triangles, a list of collocation points with their indices, a list of geometric nodes, interpolation functions for surface data and interpolation functions for the geometry. For an isoparametric element, the interpolation functions for the geometry are the same as those for the surface data and the geometric nodes are the same as the collocation points. This approach allows nodes to be indexed independently on each element, to support discontinuities, while allowing the underlying GTS surface to be geometrically valid.

Figure 1 shows the triangular elements which have been implemented; quadrilateral elements have also been implemented using the same approach. The shape functions employed are polynomials and elements of order zero to three have been developed. Figure 1 shows each element with its underlying GTS triangles and the collocation points. In the case of a zero order element, there is one collocation point,

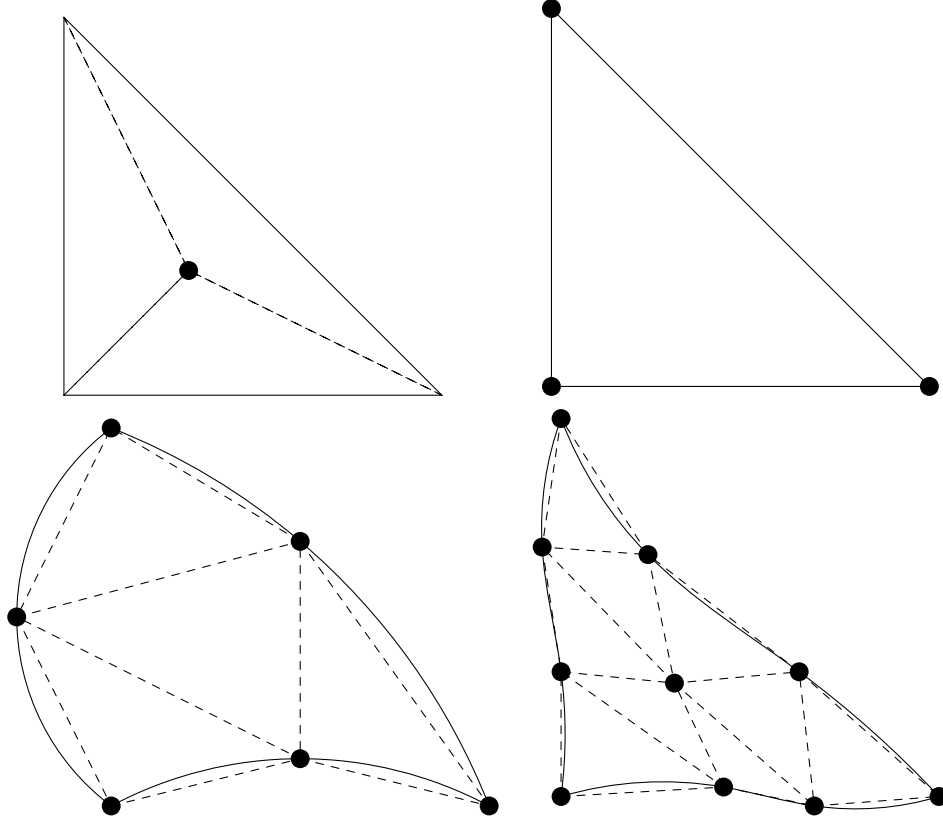


Figure 1: Triangular element types: zero, first, second and third order: circles show computational nodes, solid lines the element boundary and dashed lines the GTS triangles.

placed at the centre of the triangular element. The element is made up of three GTS triangles in order to allow for a constant solution across the computational triangle. In the case of a linear element, the computational triangle coincides with a GTS triangle and likewise the collocation points. For the second and third order elements, the element does not coincide with GTS triangles due to the element curvature, with the underlying triangles being formed by joining the collocation points with straight line segments.

Finally, a mesh is implemented as a GTS surface supplemented with a list of elements, a lookup table connecting elements to triangles and a lookup table connecting collocation points to their indices. These lookup tables are implemented as hash tables, a well-known method for efficient referencing of data.

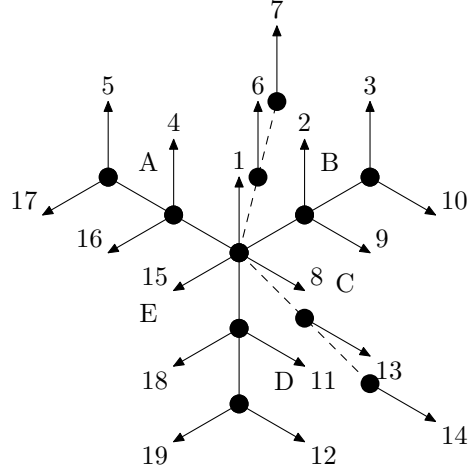


Figure 2: Renumbering the nodes at the corner of a cube

2.3 Detection and indexing of sharp edges

In order to solve problems involving general geometries, a boundary element code must have some method of dealing with sharp edges. In the case of zero-order elements where collocation points lie on one, and only one, element, there is no difficulty, but in the general case where collocation points lie on more than one element, it is required that the scheme be able to support a discontinuity in solution or boundary condition at a sharp edge. As in previous work, this is implemented by giving points of discontinuity multiple indices. This allows for a discontinuity as the sharp edge is approached. An example of such indexing, at the corner of a cube, is shown in Figure 2. Points are shown with their surface normals and their indices, while elements are labelled with capital letters. As an example of a sharp edge, nodes on the line between elements B and C each have two indices while those between elements B and A have only one: the surface is smooth at these points. The exception is the corner of the cube where the node has three indices corresponding to the three planes which meet there.

A method has been developed to automatically detect and index sharp edges and corners, an important practical point in applications such as aerodynamics [15] where the imposition of an edge condition can be difficult and will ideally be performed without user intervention. To index the nodes of a mesh, each element is visited in turn. On each element, the currently unindexed nodes are visited. If a node is shared with adjoining elements, the surface normal at the node is computed on all of the elements. If the angle between normals is less than some specified value, the

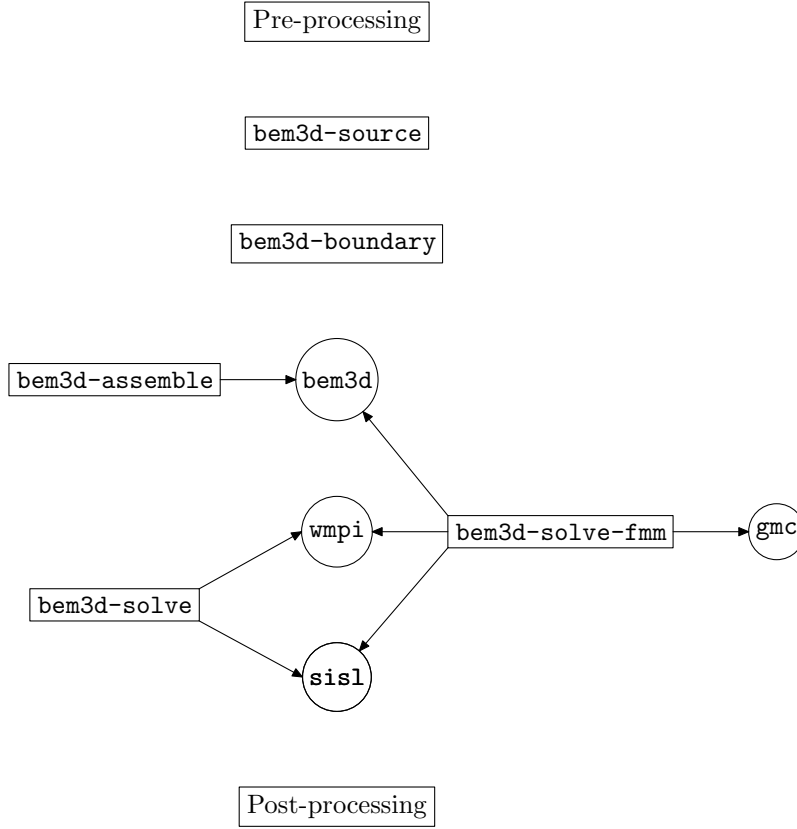


Figure 3: Structure of BEM3D codes: arrows indicate links to libraries. Executables are shown boxed and libraries circled.

surface is taken to be smooth and the node is given one index. Otherwise, it is given a different index for each normal which deviates from the reference normal by more than the specified tolerance.

2.4 Code structure

The structure of the codes in BEM3D is shown in Figure 3. The sequence shown contains all of the steps which might be needed, but in many problems they will not all be necessary. The first is a pre-processing stage to generate the geometry and elements and to index the nodes. In most cases, the geometry is generated using GMSH [4] and converted to the BEM3D format and indexed using a conversion program. Boundary conditions are then supplied, either directly, or by computing the field and its gradients from a prescribed source. If the problem is being solved

by direct solution of a matrix system, the matrices are assembled and stored to be used by the solver; if the fast multipole method is used, the information required for the matrix multiplications is generated and applied directly in the same code. If required, the field quantities can then be computed. Finally, any post-processing and visualization which might be required are performed by converting the solutions and mesh to the GMSH format.

The linkages between libraries and codes are shown in Figure 3 with executables shown boxed and libraries circled. The libraries which are used are the main BEM3D library, WMPI, a set of wrapper functions for interfacing to MPI, SISL, a simple iterative solver library and GMC, which contains the code for fast and accelerated multipole calculations.

3 ACCELERATED EVALUATION OF INTEGRALS

Since its introduction, the fast multipole method has been used by a number of workers to accelerate the boundary element and to reduce its memory requirements [16]. The standard approach of direct solution of the matrix system has time and memory requirements which scale as N^2 , which quickly exceed the resources available on even the most powerful computers. The method implemented in BEM3D allows problems to be solved directly on parallel systems using the MPI standard but it was considered better to implement a fast multipole method for solution of problems and for calculation of radiated fields. The fast multipole method was originally developed for point sources, rather than elements of finite extent, and is usually implemented using spherical harmonics. In the method implemented in BEM3D, the basic algorithm is similar to the original adaptive fast multipole method [17], but with two important differences. The first is the use of Taylor series in place of spherical harmonics, as used by Tausch in his non-adaptive method [18, 19], in order to cater for a wide variety of Green's functions. The second is a convergence radius criterion for the near field, an idea developed [20] to allow for finite size elements which may not be completely contained within a box of the tree decomposing the computational surface. The rest of this section details the sequence of procedures involved in performing a fast multipole solution of the boundary element equations.

3.1 Hierarchical domain decomposition

The first step in a fast multipole method is to recursively decompose the domain into a tree structure. The tree is made up of boxes aligned with the coordinate axes with each box containing up to eight boxes, formed by dividing the main box along each

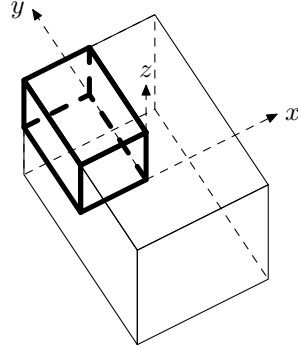


Figure 4: Decomposition of a box of points: the parent box is shown with one child box indicated in bold

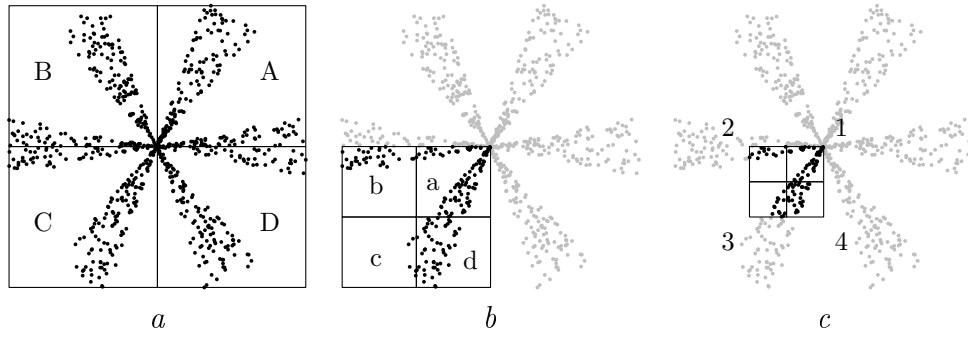


Figure 5: Decomposition of a set of points

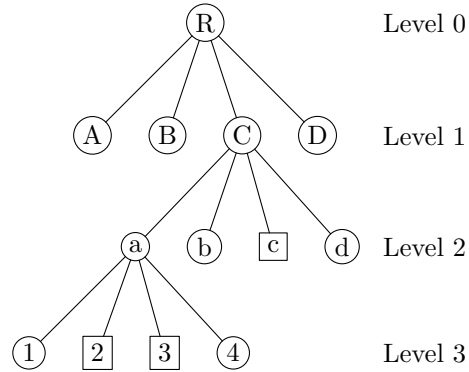


Figure 6: Tree structure for decomposition of Figure 5

of the axes, Figure 4. The main box is called a ‘parent box’ and the boxes formed by subdivision are the ‘child boxes’. The decomposition of the domain is initialized by forming a box which contains all of the vertices of the computational surface S . This box is said to be at level zero. The box is then subdivided to form the level one boxes, which are themselves divided to form the level two boxes and so on. At each stage of division, the number of vertices in a box is checked. If it is less than some prescribed number B , division of the box is terminated and the box is called a ‘leaf’. Recursive division in this manner gives rise to a tree structure where the box at each node of the tree encloses all of the boxes in the nodes below it.

The process of subdivision is shown in two dimensions in Figure 5. An initial distribution of points is enclosed by a level zero box which is divided into four level one child boxes, labelled A, B, C and D, Figure 5*a*. Following the decomposition of box C, Figure 5*b* shows the level two boxes a, b, c and d. In this case, box c has fewer than B points and is subdivided no more. Following the subdivision one more time, box a is divided into four level three boxes, 1, 2, 3 and 4, of which boxes 2 and 3 are not divided again.

Part of the resulting tree structure is shown in Figure 6, with leaf nodes of the tree shown boxed and parent nodes shown circled. The parent node R at level 0 has four child nodes, corresponding to the four boxes of Figure 5*a* and so forth. The tree structure can be used to rapidly locate a point and as the basis for fast integration methods.

The final step in generating the tree is to attach the elements of the mesh to the leaf nodes. The method adopted here is to list the elements attached to the vertices of a leaf box and link this list to the leaf node.

3.2 Taylor multipole expansions

A fast multipole method works by replacing a list of elements attached to a box with a set of multipole coefficients which can be used to compute the field due to the elements in the box far field, where ‘far field’ will be defined more precisely below. This was originally done using an expansion of the field in spherical harmonics, but here Taylor series expansions have been used since they allow the unified treatment of a range of Green’s functions [18, 19], an important point in constructing a general code.

The field integrals to be considered are of the form:

$$I(\mathbf{x}) = \int_{S_b} f(\mathbf{x}_1) G(R) dS_b, \quad (4)$$

where $f(\cdot)$ is a source term and S_b is the surface of the elements inside some box of the tree decomposing the surface S . To approximate $I(\mathbf{x})$, we expand the Green's function in a Taylor series about some point \mathbf{x}_c inside the box:

$$G(R) \approx \sum_{h=0}^H \sum_{m,n,k} (-1)^h G_{mnk} (x_1 - x_c)^m (y_1 - y_c)^n (z_1 - z_c)^k, \quad (5a)$$

$$G_{mnk} = \frac{1}{m!} \frac{1}{n!} \frac{1}{k!} \left. \frac{\partial^h G}{\partial x^m \partial y^n \partial z^k} \right|_{\mathbf{x}_1 = \mathbf{x}_c}, \quad (5b)$$

where the summation over m , n and k is taken over all values of $m + n + k = h$ and the symmetry relation $\partial G / \partial x_1 = -\partial G / \partial x$ has been used. The integral can then be rewritten:

$$f(\mathbf{x}) \approx \sum_{h=0}^H \sum_{m,n,k} (-1)^h G_{mnk} I_{mnk}, \quad (6)$$

$$I_{mnk} = \int_{S_b} f(\mathbf{x}_1) (x_1 - x_c)^m (y_1 - y_c)^n (z_1 - z_c)^k dS_b.$$

The integrations can be performed the interpolation functions on each element so that:

$$I_{mnk} = \sum_i f_i w_i^{(mnk)} \quad (7)$$

where the index i runs over all points on elements connected to the source box and $w_i^{(mnk)}$ is a weight precomputed as:

$$w_i^{(mnk)} = \int_{S_b} L_i (x_1 - x_c)^m (y_1 - y_c)^n (z_1 - z_c)^k dS_b \quad (8)$$

which is independent of the underlying Green's function and so can be stored and used in multiple problems.

To evaluate the field due to the source elements contained in a box, the Taylor series can be used in an expansion about a point \mathbf{x}'_c :

$$f(\mathbf{x}) \approx \sum_{l=0}^L \sum_{m,n,k} F_{mnk} (x - x'_c)^m (y - y'_c)^n (z - z'_c)^k$$

where the expansion coefficients F_{mnk} are computed by differentiation of Equation 6:

$$\begin{aligned} \left. \frac{\partial^{q+r+s} f}{\partial x^q \partial y^r \partial z^s} \right|_{\mathbf{x}=\mathbf{x}'_c} &\approx \sum_{h=0}^H \sum_{m,n,k} (-1)^h G_{m+q,n+r,k+s} I_{mnk}, \\ F_{qrs} &= \sum_{h=0}^H \sum_{m,n,k} (-1)^h \frac{1}{q!r!s!} G_{m+q,n+r,k+s} I_{mnk}, \end{aligned} \quad (9)$$

which can be used to generate a local expansion about the centre of one box of the field due to another box.

Two basic tools are now required which allow the multipole expansions of a tree of boxes to be used to accelerate the evaluation of the field integrals. The first is the coefficient shift operator which allows coefficients I_{mnk} evaluated about one centre to be shifted to another centre. This allows the coefficients about the centre of a parent box to be evaluated from the coefficients of its child boxes rather than having to be recomputed. Writing:

$$\begin{aligned} I'_{mnk} &= \int_S f(\mathbf{x}_1) (x_1 - x'_c)^m (y_1 - y'_c)^n (z_1 - z'_c)^k dS, \\ &= \int_S f(\mathbf{x}_1) (x_1 - x_c + (x_c - x'_c))^m (y_1 - y_c + (y_c - y'_c))^n (z_1 - z_c + (z_c - z'_c))^k dS, \end{aligned}$$

and applying the binomial theorem:

$$I'_{mnk} = \sum_{q=0}^m \sum_{r=0}^n \sum_{s=0}^k \binom{m}{q} \binom{n}{r} \binom{k}{s} (x_c - x'_c)^q (y_c - y'_c)^r (z_c - z'_c)^s I_{(m-q)(n-r)(k-s)}, \quad (10)$$

which allows the coefficients I'_{mnk} about centre \mathbf{x}'_c to be computed in terms of coefficients I_{mnk} about centre(s) \mathbf{x}_c .

The second basic tool is the expansion shift operator which shifts the expansion about one centre \mathbf{x}_c , Equation 9, to give an expansion about another centre \mathbf{x}'_c .

Writing:

$$\begin{aligned}
f(\mathbf{x}) &= \sum_{l=0}^L \sum_{m,n,k} F'_{mnk} (x - x'_0)^m (y - y'_0)^n (z - z'_0)^k, \\
&= \sum_{l=0}^L \sum_{m,n,k} F_{mnk} (x - x'_0 + (x'_0 - x_0))^m (y - y'_0 + (y'_0 - y_0))^n (z - z'_0 + (z'_0 - z_0))^k, \\
&= \sum_{l=0}^L \sum_{m,n,k} F_{mnk} \sum_{q=0}^m \sum_{r=0}^n \sum_{s=0}^k (x - x'_0)^{m-q} (x'_0 - x_0)^q (y - y'_0)^{n-r} (y'_0 - y_0)^r (z - z'_0)^{k-s} (z'_0 - z_0)^s,
\end{aligned} \tag{11}$$

from which the contribution of the original coefficients F_{mnk} to the shifted coefficients F'_{mnk} can be identified. This allows a parent box expansion to shifted to its children.

3.3 Derivatives of Green's functions

In order to compute the field due to a set of multipole coefficients, we require the derivatives of the Green's function of a problem. Tausch [18] gives a recursive algorithm which efficiently and stably generates the derivatives of a Green's function up to some required order.

Given a Green's function $G(R)$ which is a function of source-observer distance $R = |\mathbf{r}|$, $\mathbf{r} = (x, y, z)$, the function:

$$G^{(h)}(R) = \left(\frac{1}{R} \frac{\partial}{\partial R} \right)^{(h)} G(R),$$

is defined. The sequence of functions $G^{(h)}$ can be computed recursively. For the Laplace Green's function, $G = 1/4\pi R$ and:

$$G^{(0)}(R) = \frac{1}{4\pi R}, \quad G^{(h+1)} = -\frac{2h+1}{R^2} G^{(h)}(R),$$

while for the Helmholtz Green's function, $G = \exp[jkR]/4\pi R$:

$$G^{(h+1)} = -\frac{2h+1}{R^2} G^{(h)}(R) - \frac{k^2}{R^2} G^{(h-1)}(R),$$

with the correction of a typographical error in the original reference.

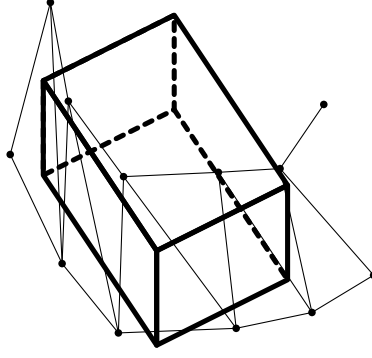


Figure 7: Elements stick out of their boxes

Given the sequence $G^{(h)}$, the derivatives of the functions with respect to the components of \mathbf{r} can be found from:

$$\frac{\partial^{m+1+n+k} G^{(h)}}{\partial x^{m+1} \partial y^m \partial z^k} = m \frac{\partial^{m-1+n+k} G^{(h+1)}}{\partial x^{m-1} \partial y^n \partial z^k} + x \frac{\partial^{m+n+k} G^{(h+1)}}{\partial x^m \partial y^m \partial z^k}, \quad (12a)$$

$$\frac{\partial^{m+n+1+k} G^{(h)}}{\partial x^m \partial y^{n+1} \partial z^k} = n \frac{\partial^{m+n-1+k} G^{(h+1)}}{\partial x^m \partial y^{n-1} \partial z^k} + y \frac{\partial^{m+n+k} G^{(h+1)}}{\partial x^m \partial y^m \partial z^k}, \quad (12b)$$

$$\frac{\partial^{m+n+k+1} G^{(h)}}{\partial x^m \partial y^n \partial z^{k+1}} = k \frac{\partial^{m+n+k-1} G^{(h+1)}}{\partial x^m \partial y^n \partial z^{k-1}} + z \frac{\partial^{m+n+k} G^{(h+1)}}{\partial x^m \partial y^n \partial z^k}. \quad (12c)$$

To compute the derivatives of the Green's function up to a given order H , Tausch gives the following scheme [18]:

1. compute $G^{(h)}$, $h = 0, \dots, H$;
2. compute $\partial^{m+n+k} G^{(h)} / \partial x^m \partial y^n \partial z^k$, for $m+n+k \leq H-h$, $h = H-1, \dots, 0$, using Equations 12;
3. set $\partial^{m+n+k} G / \partial x^m \partial y^n \partial z^k = \partial^{m+n+k} G^{(0)} / \partial x^m \partial y^n \partial z^k$, for $m+n+k = 0, \dots, H$.

3.4 Box near field

The tree decomposing the domain can be used to accelerate the computation of field integrals, using the methods described in the next two sections. The basic approach is to use the multipole expansion about a box centre to compute the field 'far' from the box and to use full integration over the box elements 'close' to the box. This requires a definition of 'near' and 'far' which can be used in deciding which procedure

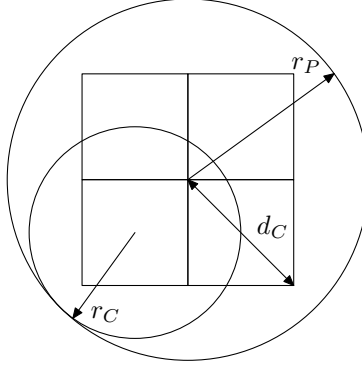


Figure 8: ‘Inheritance’ of child convergence radius r_C by parent box with convergence radius r_P

to use. In the original version of the fast multipole method [17], the point sources used were completely contained in a box and the near field of a box was defined as its neighbours. When elements of finite extent are used, they will inevitably stick out of the boxes to which they are attached and it is not clear how to define the boundary of the ‘far field’ of the box.

A number of approaches have been discussed to deal with this problem, some of them limited to zero order elements. Tausch [19] defines a separation ratio which can be used in deciding when boxes lie in each others’ near field. This has the disadvantage that it requires the boxes to be at the same level in the tree, i.e. that they be the same size. Another approach, employed in a spherical harmonic fast multipole code [20], is to use the convergence radius of the expansion about a box centre define the box near field. This approach has been used in BEM3D, with the convergence radius r_C given by the maximum distance between the box centre and a vertex of an element attached to the box (which may well not lie in the box proper). A point lies in the far field of the box if its distance to the box centre is greater than r_C . Two boxes, which need not be the same size, lie in each others’ far fields if the distance between their centres is greater than the sum of their convergence radii.

Finally, the convergence radius r_P of a parent box can be derived from the radii of its child boxes using the approach shown in Figure 8:

$$r_P = r_C + d_C/2, \quad (13)$$

where r_C is the maximum of the convergence radii of the child boxes and d_C is the length of a child box’s diagonal.

3.5 Accelerated field evaluation

The first principal application of the basic techniques of the previous sections is in accelerated evaluation of the field due to a known source distribution over a surface. Given the tree decomposition of Section 3.1, the multipole moments computed at each leaf node and shifted upwards in the tree, Section 3.2 and a field point \mathbf{x} , the field may be evaluated by traversing the tree and computing the contribution from each box of the tree in turn, descending the tree only far enough to evaluate the contribution of a branch to sufficient accuracy.

The algorithm may be summarized as follows:

1. set $I(\mathbf{x}) = 0$;
2. set the current box to the root of the tree at level 0;
3. for the current box:
 - (a) if the distance to the box centre $|\mathbf{x} - \mathbf{x}_c| > r_C$, evaluate the multipole expansion of Equation 9 and add to $I(\mathbf{x})$; terminate descent of this branch;
 - (b) if the distance to the box centre $|\mathbf{x} - \mathbf{x}_c| \leq r_C$ and the current box is a parent, repeat step 3 for each child box;
 - (c) if the distance to the box centre $|\mathbf{x} - \mathbf{x}_c| \leq r_C$ and the current box is a leaf node, evaluate the field by direct integration over the elements of the box and add to $I(\mathbf{x})$; terminate descent of this branch.

This algorithm can be used to evaluate the field at a small number of points which may be far from the surface S : it is efficient and avoids the setup costs involved in the fast multipole method proper. When the field must be evaluated at a large number of points, for matrix multiplication, say, the fast multipole method described in the next section is used.

3.6 Fast matrix multiplication

In order to further accelerate the computation of integrals in the boundary element method, the technique of the previous section can be extended to a true fast multipole method, at the expense of some extra pre-processing. This yields a method which speeds up the matrix multiplications required for the solution of the boundary element equations by using local expansions of the field about the centre of each leaf node of the tree.

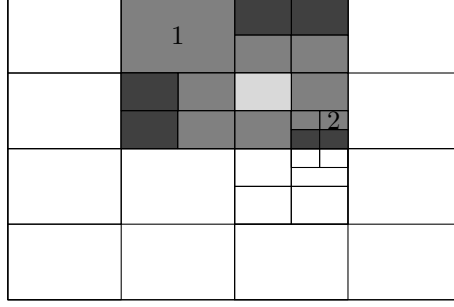


Figure 9: Interaction and near field lists for a tree box

The algorithm is similar to that of the previous section but with some extra procedures related to the evaluation of the near field terms and the separation of boxes into near and far field. The first step is, as before, to generate the tree decomposing the surface, including the multipole coefficients and convergence radii for the boxes. Each box now has linked to it two lists: the near-field list and the interaction list. The near-field list consists of boxes whose contribution to the field in the box must be computed by direct integration over the attached elements. The interaction list is made up of boxes whose contribution can be computed using the multipole expansion. Figure 9 shows an example. The light grey box in the middle of the grid is the box whose lists are shown. The darker boxes are those in the near-field list, using the criterion of Section 3.4 which states that boxes are well-separated iff:

$$|\mathbf{x}_c^{(1)} - \mathbf{x}_c^{(2)}| > r_C^{(1)} + r_C^{(2)}, \quad (14)$$

where $\mathbf{x}_c^{(i)}$ and $r_c^{(i)}$ are the centre and radius of convergence of each of the boxes. The darkest boxes are those on the interaction list whose contribution to the field in the main box can be computed using multipole expansions. The field in the box is computed as a sum of contributions from the near field and interaction list boxes and from the local expansion about the centre of the parent box which is computed in the same way. In Figure 9, the box labelled 1 is in the near field list, even though it is larger than the main box, because it is a leaf node and must contribute directly to the field. The box labelled 2 is in the near field list, even though it does not touch the main box, because it does not meet the separation criterion of Equation 14.

The near-field and interaction lists can be generated using the following algorithm, applied to each box B descending the tree starting at level zero:

1. initialize the interaction and near-field lists of B to be empty;
2. traverse the near field list of the box's parent P and for each box N in the list:

- (a) if N is a leaf node:
 - i. if N and B are well-separated, add N to the interaction list of B ;
 - ii. if N and B are not well-separated, add N to the near-field list of B ;
- (b) if N is not a leaf node, traverse the child boxes C of N and:
 - i. if C and B are well-separated, add C to the interaction list of B ;
 - ii. if C and B are not well-separated, add C to the near-field list of B ;

Given a tree with multipole coefficient weights $w^{(mnk)}$ up to order $m+n+k = H$, and near-field and interaction lists for each box, a matrix multiplication can be performed as follows:

1. for each leaf box, compute the multipole moments $I_{mnk} = \sum_i f_i w_i^{(mnk)}$, $m+n+k \leq H$;
2. traverse tree from bottom to top, calculating box moments by accumulating the contribution from child boxes using Equation 10;
3. traverse tree from top to bottom, computing local expansions to order L :
 - (a) shift parent local expansion to box centre using Equation 11;
 - (b) add local expansion terms due to boxes in interaction list;

each leaf box now has an expansion about its centre which gives the field in the box due to all other boxes except those in the near-field list;

4. for each leaf box, evaluate the local expansion at each enclosed vertex and add the contribution from boxes in the near-field list.

In practice, the near-field contribution is precomputed and stored as a sparse matrix for re-use in the solution procedure and the expansion order L is a function of depth in the tree [19] in order to avoid excessively high order expansions in small boxes. The order L_l at level l is set to $L_l = \min(L_{\max}, L_{\min} + l_{\max} - l)$.

4 NUMERICAL TESTS

The performance of the boundary element codes has been assessed in terms of accuracy, speed and memory. The test uses a point source placed inside the surface to generate a potential and a boundary condition (potential gradient). The system is solved for the boundary condition which should recover the original surface potential

due to the point source. The error measure is the rms difference between the original and computed potential. Two geometries have been used, a unit sphere and a cube of edge length 2 centred on the origin. The sphere is generated by successive refinement of an initial surface, allowing tests to be carried out on a smooth surface with control over the number of vertices. The cube is generated using GMSH [4] with successively smaller edge lengths. This tests the ability of BEM3D to deal with sharp edges using the methods outlined earlier. Tests have been conducted with first and second order elements and the Laplace and Helmholtz ($k = 2$) equations have been solved. The fast multipole method was used to solve problems of all sizes and the direct matrix method was used for the smaller problems which would fit in memory. Calculations were performed on a 3GHz Pentium 4 with 1Gb of memory.

Data reported are the number of vertices, the maximum number of vertices B in a tree box, the setup time and solution time and the maximum memory used during solution. For matrix solution, the setup time is the time required to assemble the system matrices. For the fast multipole method, the setup time is that needed to generate the tree for the mesh and compute and store the near-field matrix. In neither case is the time needed for disk storage and recovery included. In the fast multipole case, the time reported is the total setup time for one problem. In practice, because the multipole coefficient weights are independent of the problem being solved, the setup time for multipole problems could be reduced by re-using the weights. In both cases, the solution time reported is that needed for solution using the stabilized biconjugate gradient method [11].

As a reference case, the fast multipole solver uses a minimum expansion order of 3 and a maximum of 8. For larger problems, the error ceases to reduce with element size. This appears to be due to the multipole precision being larger than the discretization error. As a check, a number of the larger problems were solved with the minimum expansion order increased to 4. These results are included in the tabulated data and indicated by an asterisk.

Table 1: Code performance for Laplace equation on sphere using first order elements

N	B	FMM				Direct			
		ϵ	$t_{\text{setup}}/\text{s}$	t/s	Mb	ϵ	$t_{\text{setup}}/\text{s}$	t/s	Mb
42	8	3.03×10^{-2}	1	0	2	5.31×10^{-3}	1	0	0
162	16	1.55×10^{-2}	6	3	5	1.38×10^{-3}	5	0	2
642	32	3.48×10^{-4}	40	7	10	3.46×10^{-4}	80	0	8
2562	64	9.03×10^{-5}	473	8	49	8.62×10^{-5}	1322	0	104
2562*	64	8.59×10^{-5}	491	11	49				
10242	128	7.32×10^{-5}	1758	54	203				
10242*	128	2.96×10^{-5}	1897	70	203				

Table 2: Code performance for Laplace equation on sphere using second order elements

N	B	FMM				Direct			
		ϵ	$t_{\text{setup}}/\text{s}$	t/s	Mb	ϵ	$t_{\text{setup}}/\text{s}$	t/s	Mb
162	8	2.04×10^{-4}	5	3	5	2.03×10^{-4}	3	0	2
642	16	2.55×10^{-5}	25	7	11	2.20×10^{-5}	32	0	8
2562	32	3.33×10^{-5}	102	47	37	2.32×10^{-6}	474	0	104
10242	64	4.82×10^{-5}	749	53	193				
40962	128	8.12×10^{-5}	3611	264	842				

Table 3: Code performance for Helmholtz equation on sphere using first order elements

N	B	FMM				Direct			
		ϵ	$t_{\text{setup}}/\text{s}$	t/s	Mb	ϵ	$t_{\text{setup}}/\text{s}$	t/s	Mb
42	8	3.46×10^{-2}	1	0	2	5.14×10^{-3}	1	0	430
162	16	1.45×10^{-2}	10	20	6	1.28×10^{-3}	6	0	3
642	32	3.30×10^{-4}	68	35	12	3.15×10^{-4}	118	0	15
2562	64	1.18×10^{-4}	843	40	70	7.73×10^{-5}	1758	1	207
2562*	64	7.75×10^{-5}	1398	25	122				
10242	128	1.83×10^{-4}	3020	284	284				
10242*	128	2.06×10^{-5}	4721	231	475				

Table 4: Code performance for Helmholtz equation on sphere using second order elements

N	B	FMM				Direct			
		ϵ	$t_{\text{setup}}/\text{s}$	t/s	Mb	ϵ	$t_{\text{setup}}/\text{s}$	t/s	Mb
162	16	1.71×10^{-2}	5	9	6	3.62×10^{-4}	3	0	0
642	32	8.00×10^{-5}	31	23	14	4.30×10^{-5}	39	0	15
2562	64	9.64×10^{-5}	247	25	74	4.64×10^{-6}	583	1	206
2562*	64	7.75×10^{-5}	1398	25	122				
10242	128	1.38×10^{-4}	888	165	282				
10242*	128	2.06×10^{-5}	4721	231	475				

Table 5: Code performance for Laplace equation on cube using first order elements

N	B	FMM				Direct			
		ϵ	$t_{\text{setup}}/\text{s}$	t/s	Mb	ϵ	$t_{\text{setup}}/\text{s}$	t/s	Mb
117	5	2.22×10^{-3}	7	9	5	2.22×10^{-3}	4	0	0
431	10	4.85×10^{-4}	21	21	9	4.87×10^{-4}	30	0	5
1763	20	1.17×10^{-4}	114	81	29	1.19×10^{-4}	552	0	50
7281	40	2.55×10^{-5}	618	124	98				
28029	80	2.70×10^{-5}	5003	227	512				
28029*	80	7.85×10^{-6}	17691	391	854				

Table 6: Code performance for Laplace equation on cube using second order elements

N	B	FMM				Direct			
		ϵ	$t_{\text{setup}}/\text{s}$	t/s	Mb	ϵ	$t_{\text{setup}}/\text{s}$	t/s	Mb
378	10	1.25×10^{-4}	27	47	8	1.24×10^{-4}	10	0	4
1538	20	1.71×10^{-5}	69	69	27	5.61×10^{-6}	154	0	39
1538*	20	6.90×10^{-6}	73	94	27				
6674	40	9.10×10^{-6}	361	147	106	2.78×10^{-7}	2982	1	695
6674*	40	5.45×10^{-7}	614	279	147				
28362	80	2.09×10^{-5}	2551	253	636				

Table 7: Code performance for Helmholtz equation on cube using first order elements

N	B	FMM				Direct			
		ϵ	$t_{\text{setup}}/\text{s}$	t/s	Mb	ϵ	$t_{\text{setup}}/\text{s}$	t/s	Mb
117	5	3.46×10^{-3}	8	67	5	3.47×10^{-3}	5	0	2
431	10	7.34×10^{-4}	46	158	34	7.43×10^{-4}	37	0	8
1763	20	1.69×10^{-4}	269	489	36	1.68×10^{-4}	657	1	98
7281	40	5.11×10^{-5}	854	408	128				
28029	80	7.18×10^{-5}	6246	1142	713				

Table 8: Code performance for Helmholtz equation on cube using second order elements

N	B	FMM				Direct			
		ϵ	$t_{\text{setup}}/\text{s}$	t/s	Mb	ϵ	$t_{\text{setup}}/\text{s}$	t/s	Mb
378	10	2.49×10^{-4}	31	168	10	2.45×10^{-4}	12	0	6
1538	20	5.73×10^{-5}	81	313	34	9.12×10^{-6}	189	1	76
1538*	20	1.66×10^{-5}	87	421	34				
6674	40	2.51×10^{-5}	431	1149	147				
6674*	40	1.35×10^{-6}	775	1672	205				
28362	80	5.36×10^{-5}	3009	901	892				

The first data presented are for the Laplace equation solved on a sphere, Tables 1 and 2. The number of points increases by a factor of about four between test cases and the computing demands increase at the expected rate, with the memory requirement scaling roughly as N^2 for the matrix solution and roughly linearly for the fast multipole method. This is also true for the setup time but not for the solution time, which for the matrix method is less than one second in all cases while it increases roughly linearly for the fast multipole method. For the smaller problems $N \leq 2562$, the error is essentially the same for both solution methods but beyond this point the error from the fast multipole method stops falling. This behaviour can be cured by increasing the minimum expansion order as shown by the test cases marked with an asterisk in Table 1 where the reduction in error with N has been restored. It can also be noted that, even without re-using multipole weights, the setup time for the fast multipole method is much less than that for the direct solver, far outweighing any advantage in solution time for the direct method, even for relatively small problems.

The solvers behave similarly when applied to the Helmholtz problem. The decline in error with N is similar, with a need to increase the minimum expansion order at large $N \geq 2562$.

The second test case for the Laplace and Helmholtz solvers is that of a cube of edge length two, used to check the performance of the solver on a geometry with sharp edges, a type of problem known to be quite ill-conditioned. In the case of the Laplace equation, Tables 5 and 6, the fast multipole solver is comparable in accuracy to the direct method, with the caveat that the minimum expansion order must be increased for the larger problems, but is far superior in time and memory consumption. Likewise, the results for the Helmholtz equation show the expected reduction in error with vertex number N and a much lower setup time for the fast multipole method, although the solution time is rather large for small N using second order elements. This appears to be due to the inherent ill-conditioning of the problem and because the ratio of edge vertices to non-edge vertices is greater for smaller problems. No attempt was made to optimize the mesh to improve the handling of sharp edges, as in other studies [19], since it is intended that BEM3D be able to handle unstructured meshes produced by a standard mesh generator, without requiring intervention from the user.

5 CONCLUSIONS

A new library has been developed for the boundary element solution of general problems. The library is free software released under the GNU General Public Licence. It incorporates a new adaptive fast multipole method for boundary element problems

which gives comparable accuracy to direct matrix solution at a much lower cost in terms of time and memory, making possible the solution of problems which would otherwise be too large to solve with the available resources. It includes higher order elements and has provision for the addition of user-defined elements and Green's functions without extensive recoding.

Development of BEM3D continues with the intention of adding further element types and a parallel implementation of the fast multipole method.

References

- [1] Stephane Popinet. GTS: GNU Triangulated Surface library. <http://gts.sourceforge.net/>, 2000–2004.
- [2] Mark Galassi, Jim Davies, James Theiler, Brian Gough, Gerard Jungman, Michael Booth, and Fabrice Rossi. *GNU Scientific Library Reference Manual*. Network Theory Ltd, Bristol, United Kingdom, 2005.
- [3] E. Anderson, Z. Bai, C. Bischof, S. Blackford, J. Demmel, J. Dongarra, J. Du Croz, A. Greenbaum, S. Hammarling, A. McKenney, and D. Sorensen. *LAPACK Users' Guide*. Society for Industrial and Applied Mathematics, Philadelphia, PA, third edition, 1999.
- [4] Christophe Geuzaine and Jean-François Remacle. Gmsh: a three-dimensional finite element mesh generator with built-in pre- and post-processing facilities. *International Journal for Numerical Methods in Engineering*, 2009.
- [5] Luigi Morino. Boundary integral equations in aerodynamics. *Applied Mechanics Reviews*, 46(8):445–466, 1993.
- [6] A. D. Pierce. *Acoustics: An introduction to its physical principles and applications*. Acoustical Society of America, New York, 1989.
- [7] Miguel C. Junger and David Feit. *Sound, structures, and their interaction*. Acoustical Society of America, 1993.
- [8] Michael A. Khayat and Donald R. Wilton. Numerical evaluation of singular and near-singular potential integrals. *IEEE Transactions on Antennas and Propagation*, 53(10):3180–3190, October 2005.

- [9] Ken Hayami. Variable transformations for nearly singular integrals in the boundary element method. *Publications of the Research Institute for Mathematical Sciences*, 41:821–842, 2005.
- [10] S. Wandzura and H. Xiao. Symmetric quadrature rules on a triangle. *Computers and Mathematics with Applications*, 45:1829–1840, 2003.
- [11] R. Barrett, M. Berry, T. F. Chan, J. Demmel, J. Donato, J. Dongarra, V. Eijkhout, R. Pozo, C. Romine, and H. Van der Vorst. *Templates for the solutions of linear systems: Building blocks for iterative methods*. SIAM, Philadelphia, PA, USA, 1994.
- [12] Panagiota Pantazopoulou. *Boundary integral methods for acoustic scattering and radiation*. PhD, University of Bath, Claverton Down, Bath BA2 7AY, England, 2006.
- [13] Panagiota Pantazopoulou and Michael Carley. Acoustic scattering from a wing in non-uniform flow. *Journal of Sound and Vibration*, Submitted 2006.
- [14] Panagiota Pantazopoulou, Henry Rice, and Michael Carley. Boundary integral methods for scattering in non-uniform flows. Number AIAA paper 2005-2985. AIAA, AIAA, 2005.
- [15] David J. Willis, Jaime Peraire, and Jacob K. White. A combined pFFT-multipole tree code, unsteady panel method with vortex particle wakes. *International Journal for Numerical Methods in Fluids*, 53:1399–1422, 2007.
- [16] N. Nishimura. Fast multipole accelerated boundary integral equation methods. *Applied Mechanics Reviews*, 55(4):299–324, July 2002.
- [17] H. Cheng, L. Greengard, and V. Rokhlin. A fast adaptive multipole algorithm in three dimensions. *Journal of Computational Physics*, 155:468–498, 1999.
- [18] Johannes Tausch. The fast multipole method for arbitrary Green’s functions. In Z. Chen, R. Glowinski, and K. Li, editors, *Current Trends in Scientific Computing*, pages 307–314. American Mathematical Society, 2003.
- [19] Johannes Tausch. The variable order fast multipole method for boundary integral equations of the second kind. *Computing*, 72:267–291, 2004.

- [20] André Buchau, Wolfgang Hafla, Friedemann Groh, and Wolfgang M. Rucker. Improved grouping scheme and meshing strategies for the fast multipole method. *COMPEL: The International Journal for Computation and Mathematics in Electrical and Electronic Engineering*, 22(3):495–507, 2003.